ChemComm

COMMUNICATION

View Article Online
View Journal | View Issue

Cite this: *Chem. Commun.*, 2024, **60**, 14109

Received 9th October 2024,
Accepted 25th October 2024

DOI: 10.1039/d4cc05336b

rsc.li/chemcomm

Supramolecular self-sorting predicted by a simple harmonic oscillator model†

Adriana Sacristán-Martín, ‡[a] Nerea Álvarez-Llorente, ‡[b] Eric Masson, *[c] Alberto Diez-Varga *[b] and Héctor Barbero *[b]

Macrocycles that encapsulate two guests can self-sort those into homo- and heterodimers. We report here a family of self-sorting homobimetallic Pt(II) terpyridyl acetylide dimers secured together with a pair of Cucurbit[8]uril macrocycles (CB[8]). The rigid bridging unit between both Pt centers introduces varying "hinge" angles, resulting in disparities in Pt–Pt distances in the heterodimers, and leads to recognition motif mismatch. We found that the self-sorting process can be quantified using a simple model, in which each complex behaves as a simple harmonic oscillator, whose heteroassembly tends to minimize geometry distorsions through C(aryl)–C≡C–Pt axis deformation.

Cucurbit[*n*]urils (CB[*n*]s) are barrel-shaped macrocycles consisting of *n* glycoluril units connected *via* methylene bridges. Their capacity to form strong inclusion complexes in aqueous media, primarily due to the release of energetically constrained water molecules, has established them as key components for self-sorting in a wide variety of chemical systems.[1–7] CB[8] is capable of bringing together up to two hydrophobic guests, allowing homo/hetero pair formation.[7–10] In those tertiary assemblies, cationic units on the guest tend to minimize electrostatic repulsion with the other positive guest, while maximizing attractive interaction with both carbonyl rims, resulting in head-to-tail (HT) assemblies. Nonetheless, these two driving forces might be overcome by employing square planar Pt(II)-terpyridine (tpy) complexes, wherein both extended dispersive ligand attractive forces and metallophilic interactions cooperate to exclusively afford head-to-head (HH) assemblies.[11] This new arrangement has led to several applications in peptide engineering[12,13] and hydrogen photoreduction.[14]

Homobimetallic Pt(II) acetylide complexes form quaternary assemblies upon encapsulation with two CB[8] hosts (Scheme 1). The self-sorting process can be quantified using equilibrium (1)[15] and the corresponding free energy term ΔG (eqn (2)),§ where A and B are guests, AA and BB homo-quaternary complexes, AB (or BA) hetero-quaternary complexes and $[AB]_{tot}$ is the total concentration of hetero-complex.

$$\tfrac{1}{2}AA + \tfrac{1}{2}BB \rightleftarrows \tfrac{1}{2}AB + \tfrac{1}{2}BA \quad (1)$$

$$\Delta G = -RT\ln\frac{[AB]_{tot}}{2[AA]^{\frac{1}{2}}[BB]^{\frac{1}{2}}} \quad (2)$$

The equilibrium is considered fully social when the homodimers cannot be detected by NMR spectroscopy (*i.e.* less than 1%);

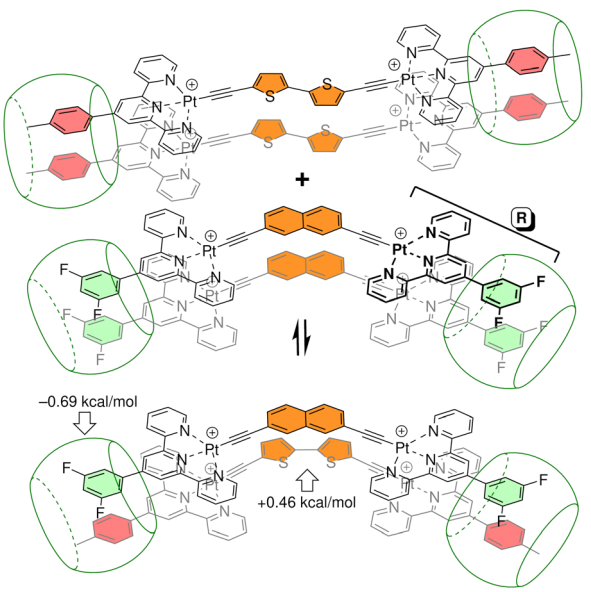

Scheme 1 Previously reported equilibrium between two homoquaternary inclusion complexes (HH) with tolyl and 3,5-difluorophenyl heads as recognition motifs.[16]

[a] *Institute of Organic Chemistry, Ulm University, 89081 Ulm, Germany*
[b] *GIR MIOMeT, IU CINQUIMA/Química Inorgánica, Facultad de Ciencias, Universidad de Valladolid, Valladolid, E47011, Spain. E-mail: alberto.diez.varga@uva.es, hector.barbero@uva.es*
[c] *Department of Chemistry and Biochemistry, Ohio University, Athens, Ohio 45701, USA. E-mail: masson@ohio.edu*

† Electronic supplementary information (ESI) available: Detailed synthetic methods and characterization. Self-sorting process study. Computational data. See DOI: https://doi.org/10.1039/d4cc05336b

‡ These two authors contributed equally to this work.

this corresponds to a −2.3 kcal mol^{-1} free energy term. Similarly, self-sorting is fully narcissistic when ΔG > +2.3 kcal mol^{-1}. In the case of bimetallic Pt(II) acetylides, self-sorting properties primarily depend on (1) the relative binding free energies of the aryl head groups; and (2) the relative orientation of the bridging group.[16] In order to isolate the second contribution, we use here rigid spacers to assess the importance of structural flexibility on self-sorting.

A family of five homobimetallic Pt(II)-tpy complexes **1–5** bearing distinct aromatic bridging ligands have been synthesized (Fig. 1). These species are expected to form well-defined homoquaternary assemblies whose self-sorting will be evaluated. To avoid the contribution of the aryl heads, a uniform tpy head group (3,5-difluophenyl) was utilized (see highlighted R group in Scheme 1); self-sorting is thus solely governed by interactions and angle mismatches between the central bridging units. The angle of bridging ligands (that we call "hinge" angle) is defined by two vectors extending from the quaternary carbons bearing the alkynyl moiety and the opposite quaternary (*para*) carbons. The range spans 64 degrees (see Fig. 1).¶ The distance between both substituted carbons in the spacer group is similar so that a good overlap is expected, with the exception of the 2,7-substituted naphthyl unit[16] (complex **5**, Fig. 1), whose length is significantly shorter than any other ligand. This spacer group has been studied to account for ligand length differences when the angle disparity is small (6°) in combination with complex **4**. In any mixture, a tpy head group mismatch (*i.e.* aryl units from distinct complexes that are misaligned within the CB[8] cavity) is therefore expected. This results in the deformation of both complexes in the heteroquaternary assembly to align both pairs of head groups; the deformation would occur at the most flexible part of the molecule, *i.e.* the acetylide moiety.[7,8,17,18] Hence, experimental free energy terms on our self-sorting scale[15] provide a measurement of Pt-alkynyl flexibility.

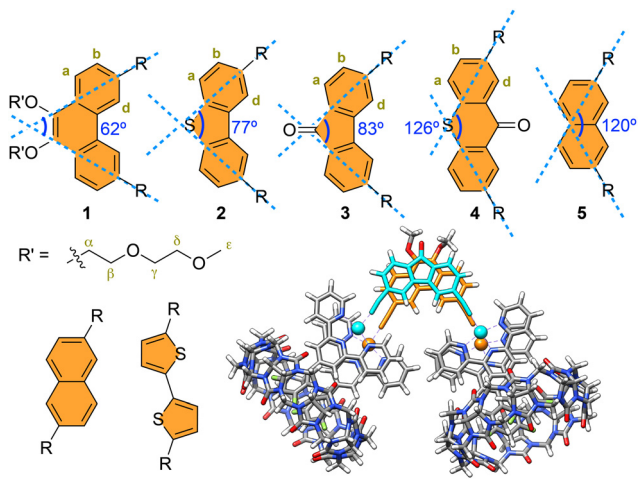

Fig. 1 Novel complexes (**1–5**) synthesized in this work along with their "hinge" angle definition.¶ Oligo(ethylene glycol) chains have been grafted to compound **1** to increase its solubility. Previously reported homobimetallic Pt-tpy complexes.[16] GFN2-*x*TB optimized structure of assembly **3**·**1**·CB[8]$_2$.‖ See Scheme 1 for the structure of group R.

Pt(II)-tpy complexes **1–4** were prepared from the corresponding diacetylide ligands, chloro-[4′-(3,5-difluoro phenyl)-2,2′:6′,2″-terpyridine]platinum(II) chloride, copper(I) iodide and isopropyl amine.§ These complexes readily formed HH homoquaternary assemblies **1**$_2$·CB[8]$_2$–**4**$_2$·CB[8]$_2$ upon addition of 1.0 equivalent of CB[8] to their suspension in a 2 : 1 mixture of D_2O and CD_3CN (Fig. S91–S114, ESI†).§ Pairs of homoquaternary assemblies **1**$_2$·CB[8]$_2$–**5**$_2$·CB[8]$_2$ were then combined in equimolar amounts, and kept at 40 °C for up to 12 days until equilibrium was reached, as shown by ^{1}H- and ^{19}F-NMR spectroscopy.§ All mixtures are in slow exchange regime, allowing the observation of new (integrable) signals corresponding to the heteroquaternary assemblies formed at the expense of their homoquaternary counterparts (Fig. 2 and Fig. S122–S151, ESI†).§ All heteroquaternary assemblies could also be fully characterized by high resolution mass spectrometry (HRMS).§ The observed decline in social behaviour with increasing calculated hinge angle mismatch (or d_{Pt-Pt} difference) was expected. Most mixtures self-sort narcissistically (from +0.90 to +0.02 kcal mol^{-1}, corresponding to 18% and 49% of the heteroassembly, respectively, Table 1). A notable exception is heteroassembly **2**·**3**·CB[8]$_2$, that bears dibenzothiophene and fluorenone spacer groups, which is favoured over the corresponding pair of homoassemblies (free energy term −0.45 (±0.05) kcal mol^{-1}, *i.e.* 68% of heterodimer, Table 1). This might suggest some favourable Coulombic interactions in the heteropair of central units; the low hinge angle mismatch (6°) and very short Pt–Pt distance difference (0.22 Å) are not significant enough to cause strain in the heteroassembly. On the other hand, the mixture between assemblies **4**$_2$·CB[8]$_2$ and **5**$_2$·CB[8]$_2$, which was expected to account for distinct spacer group length (d_{Pt-Pt} difference of 2.08 Å) while keeping a nearly negligible hinge angle mismatch (6°), returns a small free energy term of +0.16 (±0.01) kcal mol^{-1}, or 43% of heteroquaternary assembly.

To rationalize these findings, we questioned whether a set of simple descriptors for each Pt complex **1–5** could be used to predict the self-sorting behaviour of any pair. To that aim, we carried out geometry optimizations with the GFN2-*x*TB[19–21] semi-empirical method§ at various constrained Pt–Pt distances.‖ Remarkably, they were found to behave as simple harmonic oscillators, as stabilities as a function of Pt–Pt distances can be fit with quadratic eqn (3), where k_a is the spring constant in

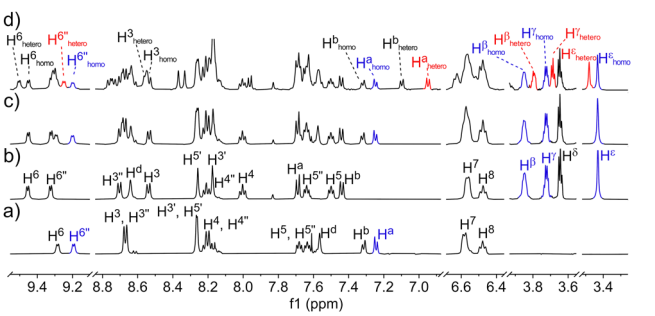

Fig. 2 Stacked ^{1}H-NMR (500 MHz, D_2O/CD_3CN 2:1) of (a) assembly **3**$_2$·CB[8]$_2$, (b) assembly **1**$_2$·CB[8]$_2$, (c) their mixture at t = 0, and (d) their mixture after 12 days.

Table 1 Free energy term ΔG [kcal mol^{-1}] for the self-sorting of Pt complexes **1–5** in the presence of CB[8]. Experiments repeated in triplicate

	1	2	3	4
2	+0.02 (±0.01)			
3	+0.07 (±0.01)	−0.45 (±0.05)		
4	+0.90 (±0.01)	+0.62 (±0.01)	+0.56 (±0.02)	
5				+0.16 (±0.01)

kcal mol^{-1} Å^{-2}, a_0 the optimal Pt–Pt distance, and a the Pt–Pt distance in the constrained systems (Fig. 3). The spring constants k' were also expressed in the more commonly used mDyn Å^{-1} unit using eqn (4), where N_A is the Avogadro constant (Table 2).

$$\Delta E = \tfrac{1}{2}k_a(a_0 - a)^2 \quad (3)$$

$$k' = 4.184 \times 10^{21}\frac{k}{N_A} = 6.948 \times 10^{-3}k \quad (4)$$

As complexes **1–5** behave like simple harmonic oscillators along a Pt–Pt axis, we then questioned whether self-sorting was simply governed by the deformation of the pair of oscillators when forced to stack on top of one another upon CB[8] encapsulation of the tpy head groups. In that case, a harmonic correlation should be observed between the free energy terms of the self-sorting process and the differences in Pt–Pt distances between the complexes. Remarkably, this is indeed the case (Fig. 4, R^2 = 0.997), with the exception of complex **2**·**3**·CB[8] that self-sorts socially (Table 1, red dot in Fig. 4). One can readily notice that major mismatches in Pt–Pt distances (up to 5.0 Å) or hinge angles (up to 64°) still allow the formation of hetero-assemblies; free energy terms of the self-sorting processes do not exceed +0.90 kcal mol^{-1}. Yet, Fig. 3 shows that compressing or expanding the Pt–Pt distance in complexes **1–5** does result in significant destabilization (0.6–2.3 kcal mol^{-1} for 1 Å distortions). Distortions imposed to Pt complexes to reach identical Pt–Pt distances in hetero-quaternary assemblies can be calculated using eqn (5)–(7) and the following hypothesis: the distortion energy ΔE_{hetero} is modelled as the sum of the harmonic oscillator of both

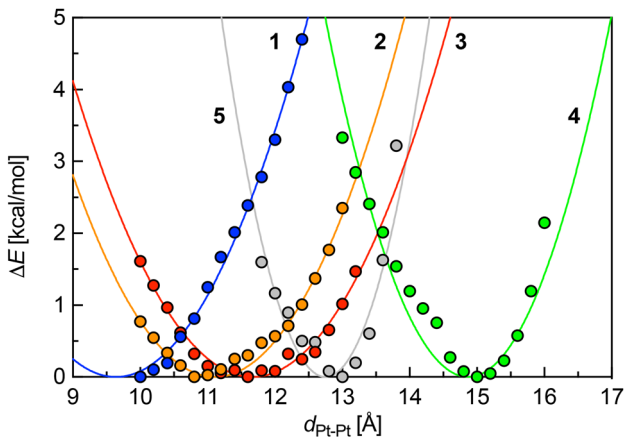

Fig. 3 Energy profiles [kcal mol^{-1}] of Pt complexes **1–5** as a function of Pt–Pt distance [Å] (electronic component at 0 K relative to the optimized relaxed structure).

Table 2 Physical parameters of complexes **1–5** when treated as harmonic oscillators

	Hinge angle [°]	d_{Pt-Pt} [Å]	k [kcal mol^{-1} Å^{-2}]	k' [mDyn Å^{-1}]
1	62	10.21	1.22 (±0.07)	8.5 (±0.5) × 10^{-3}
2	77	11.23	1.26 (±0.05)	8.7 (±0.4) × 10^{-3}
3	83	11.45	1.16 (±0.04)	8.0 (±0.3) × 10^{-3}
4	126	15.24	2.3 (±0.2)	1.6 (±0.1) × 10^{-2}
5	120	13.16	4.6 (±0.5)	3.2 (±0.3) × 10^{-2}

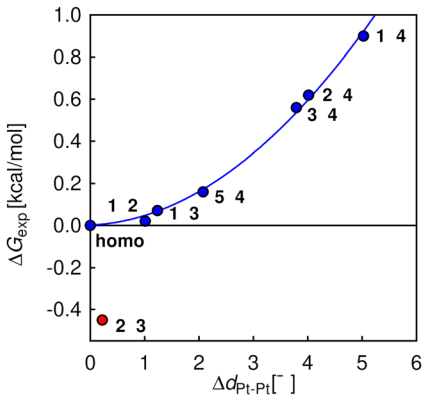

Fig. 4 Free energy terms for self-sorting processes between pairs of Pt complexes **1–5**, as a function of their Pt–Pt distance mismatches. Harmonic correlation (blue line); outlier in red; "*n*·*n*" refers to all pairs of identical Pt complexes (returning ΔG = 0).

Pt complexes, where k_a and k_b are the spring constants (eqn (5)), a and b the Pt–Pt distances in the distorted hetero-quaternary assemblies, and a_0 and b_0 the distances in the optimized (relaxed) Pt complexes. With both Pt–Pt distances forced to be equal in the hetero-quaternary complexes (*i.e.* $a = b$, Fig. 5), eqn (5) and (6) afford the Pt–Pt distances that minimize the energetic penalty ΔE_{hetero} as shown in eqn (7) (Tables 3 and 4, top half).

$$\Delta E_{hetero} = \tfrac{1}{2}k_a(a - a_0)^2 + \tfrac{1}{2}k_b(b - b_0)^2 \quad (5)$$

$$\frac{d\Delta E_{hetero}}{da} = 0 \quad (6)$$

$$a = b = \frac{k_a a_0 + k_b b_0}{k_a + k_b} \quad (7)$$

The comparison of experimental self-sorting energy terms (Table 1) with the much higher calculated penalties imposed to match Pt–Pt distances in the hetero-complexes (Table 3) clearly shows that Pt–Pt distances do not need to be equal to allow hetero-quaternary assembly formation. In other terms, CB[8] encapsulation of the tpy heads remains highly favourable

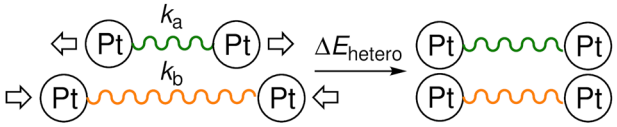

Fig. 5 Extension and contraction imposed to a pair of Pt–Pt harmonic oscillators to reach even lengths.

Table 3 Energy penalty in kcal mol^{-1} required to match Pt–Pt distances in hetero-quaternary assemblies of Pt complexes **1–5** in the presence of CB[8]

	1	2	3	4
2	+0.31			
3	+0.48	+0.02		
4	+5.31	+3.57	+2.77	
5				+1.67

Table 4 Top half: proposed average Pt–Pt distortion [Å] of Pt complexes **A** upon quaternary CB[8]-secured complex formation with Pt complex **B** with identical Pt–Pt distances in the hetero-complexes, based on eqn (5)–(7). Bottom half: Proposed average Pt–Pt distortion [Å] of Pt complexes **A** upon quaternary CB[8]-secured complex formation with Pt complex **B**, based on eqn (8)–(11)

B	**1**	**2**	**3**	**4**	**5**
A					
1	0	+0.51	+0.60	+3.29	
2	−0.49	0	[a]	+2.60	
3	−0.63	[a]	0	+2.53	
4	−1.73	−1.41	−1.26	0	−1.38
5				+0.70	0
1	0	+0.13	+0.24	+0.98	
2	−0.13	0	[a]	+0.80	
3	−0.25	[a]	0	+0.80	
4	−0.52	−0.43	−0.40	0	−0.30
5				+0.15	0

[a] Social self-sorting observed experimentally; model not applicable.

despite significant geometrical mismatches between the complexes. We therefore propose the following model to estimate the Pt–Pt distortions Δa and Δb in the hetero assemblies: from eqn (8) (equivalent to eqn (5), with ΔG_{exp} being the experimental self-sorting energy term), the difference between both distortions is minimized to extract both Δa and Δb terms (eqn (9)–(11)).§ Table 4 (bottom half) shows that required Pt–Pt distance distortions in the hetero assemblies are only 30 (±1)% of what they would otherwise have to be to match Pt–Pt distances (Table 4, top half, and Fig. S154 and S155, ESI†).

$$\Delta G_{exp} = \tfrac{1}{2}k_a\Delta a^2 + \tfrac{1}{2}k_b\Delta b^2 \quad (8)$$

$$D = \Delta a - \Delta b \quad (9)$$

$$\frac{dD}{d\Delta a} = 0 \quad (10)$$

$$\Delta a = \sqrt{\frac{2k_b\Delta G_{exp}}{k_a(k_a+k_b)}},\ \Delta b = \sqrt{\frac{2k_a\Delta G_{exp}}{k_b(k_a+k_b)}} \quad (11)$$

In summary, we showed that two CB[8] units can readily secure hetero-pairs of Pt complexes **1–5**, despite major structural differences between the Pt complexes. While Pt arylacetylides are flexible along their C(aryl)–C≡C–Pt axis, it is the tolerance of CB[8] for the orientation and position of the encapsulated aryl tpy head groups that drives the assembly. Self-sorting can be quantified using a harmonic oscillator model based on Pt–Pt distance mismatches, predicting most self-sorting patterns. However, the model is limited, as short Pt–Pt distance mismatches may introduce favourable coulombic interactions between compatible spacer groups that promote social behaviour. Ongoing studies are addressing this limitation.

We thank the Spanish Ministry of Science and Innovation (PID2021-124691NB-I00, funded by MCIN/AEI/10.13039/501100011033/FEDER, UE). EM is grateful to the National Science Foundation (grants CHE-1507321 and CHE-1905238), the American Chemical Society Petroleum Research Fund (grant 56375-ND4), the Roenigk Family Foundation and Ohio University for their continuing financial support. A. S.-M. acknowledges support from Fundación Ramón Areces for a Postdoctoral fellowship. N. A.-L. acknowledges the University of Valladolid and Santander Bank for a predoctoral contract. A. D.-V. acknowledges the Ministerio de Universidades and the European Union – NextGenerationEU for the María Zambrano contract (ADV, CONVREC-2021-264).

Data availability

All synthetic and analytical data is provided in the ESI.† All details about mathematical and computational methods, including associated coordinates are available in the ESI.†

Conflicts of interest

There are no conflicts to declare.

Notes and references

§ See ESI† for further discussions and details.
¶ According to crystal structures obtained from the Cambridge Structural Database (CSD).
‖ We must note that the Pt–Pt distances in the hetero-quaternary complexes presented herein should be seen as average distances from a large ensemble of conformers with similar energies but varying geometries; for example, the mere rotation of the CB[8]-bound aryl substituents at position 4′ of the tpy ligand clockwise or counterclockwise relative to the tpy planes yields at least 4 different hetero-quaternary assemblies with similar stabilities but different Pt–Pt distances. Reported optimized structures only represent one of these arrangements.

1 S. Liu, *et al.*, *J. Am. Chem. Soc.*, 2005, **127**, 15959–15967.
2 J. Lagona, *et al.*, *Angew. Chem., Int. Ed.*, 2005, **44**, 4844–4870.
3 E. Masson, *et al.*, *RSC Adv.*, 2012, **2**, 1213–1247.
4 S. J. Barrow, *et al.*, *Chem. Rev.*, 2015, **115**, 12320–12406.
5 K. I. Assaf and W. M. Nau, *Chem. Soc. Rev.*, 2015, **44**, 394–418.
6 J. Murray, *et al.*, *Chem. Soc. Rev.*, 2017, **46**, 2479–2496.
7 X. Yang, *et al.*, *Angew. Chem., Int. Ed.*, 2020, **59**, 21280–21292.
8 G. Wu, *et al.*, *J. Am. Chem. Soc.*, 2022, **144**, 14962–14975.
9 G. Wu, *et al.*, *Chem. Sci.*, 2020, **11**, 812–825.
10 G. Wu, *et al.*, *Angew. Chem., Int. Ed.*, 2020, **59**, 15963–15967.
11 K. Kotturi and E. Masson, *Chem. – Eur. J.*, 2018, **24**, 8670–8678.
12 H. Barbero, *et al.*, *J. Am. Chem. Soc.*, 2020, **142**, 867–873.
13 H. Barbero and E. Masson, *Chem. Sci.*, 2021, **12**, 9962–9968.
14 R. Rabbani, *et al.*, *Chem. Sci.*, 2021, **12**, 15347–15352.
15 M. Raeisi, *et al.*, *J. Am. Chem. Soc.*, 2018, **140**, 3371–3377.
16 N. A. Thompson, *et al.*, *Chem. Commun.*, 2019, **3**, 12160–12163.
17 P. S. Bols and H. L. Anderson, *Acc. Chem. Res.*, 2018, **51**, 2083–2092.
18 K. Miki and K. Ohe, *Chem. – Eur. J.*, 2020, **26**, 2529–2575.
19 S. Grimme, *et al.*, *J. Chem. Theory Comput.*, 2017, **13**, 1989–2009.
20 C. Bannwarth, *et al.*, *J. Chem. Theory Comput.*, 2019, **15**, 1652–1671.
21 C. Bannwarth, *et al.*, *Wiley Interdiscip. Rev. Comput. Mol. Sci.*, 2021, **11**, e1493.

